



Available online at [www.sciencedirect.com](http://www.sciencedirect.com)  
**jmr&t**  
Journal of Materials Research and Technology  
journal homepage: [www.elsevier.com/locate/jmrt](http://www.elsevier.com/locate/jmrt)



## Original Article

# Efficient and inexpensive MPCVD method to synthesize $\text{Co}_3\text{O}_4/\text{MoS}_2$ heterogeneous composite materials with high stability for supercapacitors



Yu Duan <sup>a,c</sup>, Shuanglong Feng <sup>b</sup>, Shenghui Guo <sup>a</sup>, Jiyun Gao <sup>a,d,\*</sup>,  
Jiajia Qiu <sup>e</sup>, Li Yang <sup>a,\*\*</sup>

<sup>a</sup> Faculty of Metallurgical and Energy Engineering, Kunming University of Science and Technology, Kunming, 650093, China

<sup>b</sup> Micro-nano Manufacturing and System Integration Center, Chongqing Institute of Green and Intelligent Technology, Chinese Academy of Sciences, Chongqing, 400714, China

<sup>c</sup> Centre for Advanced Thin Films and Devices, School of Materials and Energy, Southwest University, Chongqing, 400715, China

<sup>d</sup> School of Chemistry and Environment, Yunnan Minzu University, Kunming, 650093, China

<sup>e</sup> Institute of Physics and IMN MacroNano, Ilmenau University of Technology, Ilmenau, Germany

---

## ARTICLE INFO

### Article history:

Received 13 September 2020

Accepted 26 December 2020

Available online 31 December 2020

---

### Keywords:

$\text{Co}_3\text{O}_4$

$\text{MoS}_2$

Core–shell heterogeneous structure

MPCVD

Supercapacitor

---

## ABSTRACT

Large-sized metal oxide particles have the potential to constitute cheap, high-performance, and high-stability supercapacitor electrode materials. Herein, the marketable large-sized  $\text{Co}_3\text{O}_4$  particles ( $\sim 6 \mu\text{m}$ ) as the starting raw material, inexpensive  $\text{Co}_3\text{O}_4/\text{MoS}_2$  core–shell heterogeneous composites have been one-step fabricated via an improvised MPCVD system modified by a domestic microwave oven. After that, the surface morphology, composition structure, and valence state of elements were analyzed to the confirmed successful synthesis of  $\text{MoS}_2$  on the surface of  $\text{Co}_3\text{O}_4$ . Besides, the performance was tested by cyclic voltammetry and galvanostatic charge–discharge method. The results show that the synergistic effect of  $\text{Co}_3\text{O}_4$  core and  $\text{MoS}_2$  shell can effectively improve the material's electrochemical performance. The specific capacitance of  $\text{Co}_3\text{O}_4/\text{MoS}_2$  composite can reach  $337 \text{ F g}^{-1}$  with a current density of  $0.5 \text{ A g}^{-1}$ , which is six times more than the raw  $\text{Co}_3\text{O}_4$  powder. Furthermore, it could maintain 93.6% of the initial specific capacitance after 2000 charges and discharges. Finally, the mechanism of material performance improvement is proposed.

© 2020 The Author(s). Published by Elsevier B.V. This is an open access article under the CC BY-NC-ND license (<http://creativecommons.org/licenses/by-nc-nd/4.0/>).

---

\* Corresponding author.

\*\* Corresponding author.

E-mail addresses: [jiyungao89@163.com](mailto:jiyungao89@163.com) (J. Gao), [yanglikmust@163.com](mailto:yanglikmust@163.com) (L. Yang).

<https://doi.org/10.1016/j.jmrt.2020.12.101>

2238-7854/© 2020 The Author(s). Published by Elsevier B.V. This is an open access article under the CC BY-NC-ND license (<http://creativecommons.org/licenses/by-nc-nd/4.0/>).

## 1. Introduction

The global energy problem is increasingly prominent and has been one of the world [1,2]. Researchers have made great efforts in energy conversion and storage. As a new generation of energy storage devices, supercapacitors have been attracting continuous attention due to their high power density, fast charging/discharging rate, and long service life [3–5].  $\text{Co}_3\text{O}_4$  was used in pseudocapacitor due to its high theoretical specific capacity ( $3560 \text{ F g}^{-1}$ ) and ideal pseudocapacitance characteristics [6,7]. However, due to the massive volume expansion/contraction, low conductivity, and polarization, the practical efficiency of  $\text{Co}_3\text{O}_4$  is far lower than the theoretical maximum, which hinders its application and development [8,9]. Also, people pay more attention to nanomaterials' research of nano-sized  $\text{Co}_3\text{O}_4$  due to its high reactivity. However, the high cost and the instability in the reaction process have been hindering their practical application. In contrast, large-scale materials with low prices, high stability, and easier practical application have been ignored by researchers. This study is focused on the development of massive  $\text{Co}_3\text{O}_4$  particles in the actual use of supercapacitors.

Building composite system is considered as an effective strategy to solve the problems of  $\text{Co}_3\text{O}_4$  in energy storage [10–12]. As we all know, carbon materials are widely used in the research of building composite materials with  $\text{Co}_3\text{O}_4$ , such as carbon/ $\text{Co}_3\text{O}_4$  [13–15], CNTs/ $\text{Co}_3\text{O}_4$  [16,17], graphene/ $\text{Co}_3\text{O}_4$  [18,19], etc. However, the theoretical capacity of carbon materials is low, which cannot meet large capacity requirements. Molybdenum disulfide ( $\text{MoS}_2$ ), as a transition metal sulfide, exhibits higher capacitance and lower energy loss than carbon. Besides, like graphite,  $\text{MoS}_2$  has a two-dimensional (2D) layered structure. The distance between adjacent layers is connected by weak van der Waals force, promoting ion insertion and extraction in charge and discharge cycle [20]. Therefore,  $\text{MoS}_2$  is often reported to be used in the construction of composite materials in energy devices. For example, Liu et al. proposed a simple in-situ hydrothermal method to synthesize  $\text{NiS}_2/\text{MoS}_2$  nanowires on nickel foam, which can be directly used as a binder-free electrode, thereby ensuring high conductivity. The electrode prepared by the 12 h hydrothermal reaction exhibited area capacitance of  $4.46 \text{ F cm}^{-2}$  at a current density of  $5 \text{ mA cm}^{-2}$  and excellent cycle stability with 8.6% capacitance loss after 3000 cycles [21]. Zhang et al. reported a new ultrasonic-assisted shearing physical method, prepared a large amount of c- $\text{MnO}_2$  into s- $\text{MnO}_2$  and then deposited  $\text{MoS}_2$  composite material magnetron sputtering to form a heterojunction structure in s- $\text{MnO}_2/\text{MoS}_2$ . The results show that the heterojunction structure in s- $\text{MnO}_2/\text{MoS}_2$  exhibits excellent performance, due to it has a large specific surface area and high conductivity. Also, an asymmetrical all-solid supercapacitor based on s- $\text{MnO}_2/\text{MoS}_2$  was fabricated. After 3000 charging and discharging processes, its specific capacitance can still maintain 90% of the cycle stability, which can better reflect the actual capacitor performance [22].

Herein, for the application of large-scale  $\text{Co}_3\text{O}_4$  powder, we propose a novel material packaging method that uses the microwave plasma chemical vapor deposition (MPCVD) method to produce large-scale ( $\sim 6 \mu\text{m}$ )  $\text{Co}_3\text{O}_4/\text{MoS}_2$  core–shell

composite. Firstly, the precursor was prepared by coating s and  $\text{MoCl}_5$  on the surface of  $\text{Co}_3\text{O}_4$  powder by the solution-drying method, and then the vertical sheet  $\text{MoS}_2$  nanoshell was synthesized on the surface of  $\text{Co}_3\text{O}_4$  by one-step MPCVD method. A domestic microwave oven modifies the experimental equipment. Compared with traditional methods, it has many advantages, such as low cost, fast speed, and simple operation. After that, the morphology, composition, and electrochemical performance of the composite materials were analyzed by various methods. The prepared  $\text{Co}_3\text{O}_4/\text{MoS}_2$  composite material has a specific capacitance of  $337 \text{ F g}^{-1}$  when the current density is  $0.5 \text{ A g}^{-1}$ . It can still maintain an initial specific capacitance of 93.6% after 2000 cycles of charge and discharge. Finally, the effect of composite microstructure on electrochemical performance is discussed in detail. Our work provides a new possibility and innovation for the efficient utilization of large-scale transition metal oxide powder, especially for the electrode of a supercapacitor with high stability. The response diagram is shown in Fig. 1.

## 2. Experimental

### 2.1. Precursor preparation

Firstly, 50 ml of  $\text{CS}_2$  solution was introduced into a mortar, and 200 mg of sulfur powder was quickly dissolved in the  $\text{CS}_2$  solution. Then mix 200 mg of  $\text{Co}_3\text{O}_4$  powder in a fully dissolved solution and stir in the air to dry. Because of the volatilization of  $\text{CS}_2$ , sulfur will be separated during the stirring process and evenly coated on the  $\text{Co}_3\text{O}_4$  powder surface. After the powder sample was dried entirely, 400 mg of molybdenum pentachloride was dissolved in anhydrous ethanol and dropped into the powder sample for further grinding. Then put the sample into a vacuum drying oven and dissolve it at  $60^\circ\text{C}$  for drying. Finally, the precursor system is ready.

### 2.2. $\text{Co}_3\text{O}_4/\text{MoS}_2$ composite material synthesis

The prepared precursor was put into the quartz boat and then into the MPCVD quartz tube's furnace cavity. Firstly, the furnace chamber is pumped to vacuum, and then Ar is injected according to the flow rate of 350 sccm. When the pressure in the furnace cavity is stabilized, the microwave source is turned on to generate plasma, and the sample can

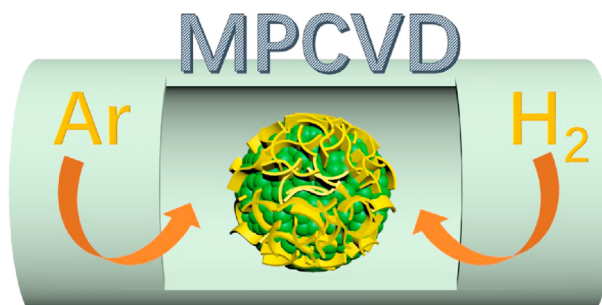


**Fig. 1 – Schematic diagram of the coating growth mechanism for the  $\text{Co}_3\text{O}_4/\text{MoS}_2$  composites.**

react at 500 °C for 10 min in the Ar plasma. After the reaction, turn off the microwave source and cool the sample to room temperature in the Ar atmosphere. Then turn off the air source and pump to vacuum before taking out the sample.

Under the heating effect of microwave plasma, S reacts with  $\text{MoCl}_5$  and eventually generates  $\text{MoS}_2$  on the surface of  $\text{Co}_3\text{O}_4$ . Simultaneously, free radicals and active groups in microwave plasma can increase reaction and accelerate the reaction rate. The chemical reaction equation for generating molybdenum disulfide is as follow:



## 2.2. Characterization method

The field emission scanning electron microscopy (FE-SEM, JSM-7800F, JEOL, Japan) was employed to observe the samples' morphology. The microstructure of the sample was expressed over the range 20°–90° by X-ray diffraction spectrum (XRD, X'Pert3 Powder, Panalytical, Netherland), Cu  $\text{K}\alpha$  radiation ( $\lambda = 1.5418 \text{ \AA}$ ). The X-ray photoemission spectroscopy (XPS, Kratos Analytical Ltd., U.K.) was used to exhibit the samples' elemental composition and valence state.

## 2.3. Fabrication of electrodes and performance measurement

The electrode's preparation process was as follows: firstly, the prepared active material, acetylene black and polyvinylidene fluoride were mixed in a ratio of 8:1:1, and then ground into slurry after adding NMP. After that, the slurry was coated on the ultrasound-treated nickel foam substrate (1 cm × 1 cm) and dried in a vacuum oven at 60 °C for 8 h. The mass of active substance on the nickel foam collecting fluid should be higher than  $1 \text{ mg cm}^{-2}$ .

The working electrode, Pt counter electrode, and Hg/HgO reference electrode constitute a three-electrode system.

Cyclic voltammograms (CV), galvanostatic charge/discharge (GCD), and cycle life were tested in 6 mol/L KOH electrolyte.

## 3. Result and discussion

SEM analyzed the surface structure of the composite. Fig. 2a and b shows the SEM images of the raw  $\text{Co}_3\text{O}_4$  and  $\text{Co}_3\text{O}_4/\text{MoS}_2$  powder, raw  $\text{Co}_3\text{O}_4$  is a spherical powder with a diameter of about 6  $\mu\text{m}$  and is composed of small particles with a diameter of about 300 nm. Moreover, there are small pores between the tiny particles. When the surface of  $\text{Co}_3\text{O}_4$  powder is coated with  $\text{MoS}_2$  shell through experiments, the morphology of composite powder becomes the appearance in Fig. 2b. The powder's surface is covered with an upright lamellar structure, namely the  $\text{MoS}_2$  shell that we synthesized on the surface of  $\text{Co}_3\text{O}_4$ . It can be observed from the specific surface area of the powder significantly increases after the flake  $\text{MoS}_2$  coated, which provides much more active sites for the energy storage, enabled the material to carry out the redox reaction more thoroughly, thus improving the electrochemical performance. Element mapping was used to analyze the distribution of elements in the  $\text{Co}_3\text{O}_4/\text{MoS}_2$  composite and the mapping results of the illustration in Fig. 2b is shown in Fig. 2c-f. It is observed that the elements of Mo, S, Co, and O are evenly distributed. Thus, we can confirm that the  $\text{MoS}_2$  layer is uniformly wrapped on the surface of  $\text{Co}_3\text{O}_4$ .

To verify the composite material's composition, the sample of  $\text{Co}_3\text{O}_4/\text{MoS}_2$  composite material was tested by X-ray diffraction to analyze its composition and crystal structure. Fig. 3 shows the XRD pattern of  $\text{Co}_3\text{O}_4/\text{MoS}_2$  composite powder in the scanning range of 10–90°. The results showed that the samples were mainly composed of three components: the diffraction peaks at 14.3° and 39.6° were corresponding to the (002) and (103) crystal planes of  $\text{MoS}_2$  (JCPDS: 37-1492). Moreover, the diffraction peaks at 31.3°, 36.8°, 44.8°, 59.3°, and 65.2° correspond to the (220), (311), (400), (511) and (440) crystal

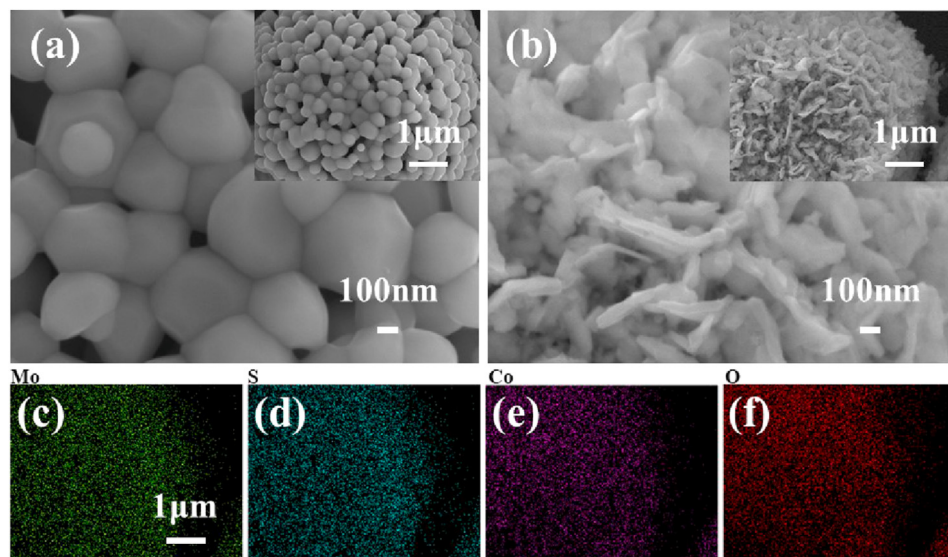


**Fig. 2 – SEM images of raw  $\text{Co}_3\text{O}_4$  powder (a),  $\text{Co}_3\text{O}_4/\text{MoS}_2$  composite (b), and the corresponding element mappings of molybdenum (c), sulfur (d), cobalt (e) and oxygen (f).**

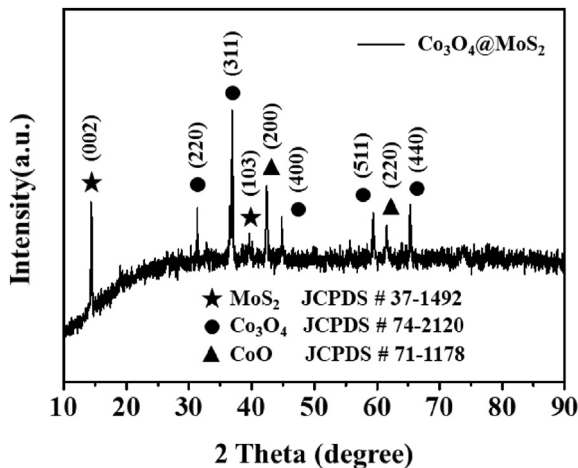


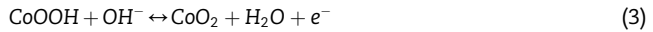
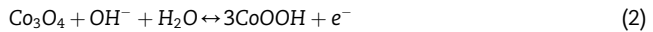
**Fig. 3 – (a) XRD pattern of the  $\text{Co}_3\text{O}_4/\text{MoS}_2$  composite.**

planes of  $\text{Co}_3\text{O}_4$  (JCPDS: 74-2120). Furthermore, the remaining diffraction peaks at  $42.4^\circ$  and  $61.5^\circ$  were consistent with the (200) and (220) crystal planes of  $\text{CoO}$  (JCPDS: 71-1178). The XRD diffraction peaks proved that  $\text{MoS}_2$  nanosheet was successfully generated on the surface of spherical  $\text{Co}_3\text{O}_4$  powder. On the other hand, the presence of  $\text{CoO}$  in the composite may be due to the collision of active groups in the microwave plasma, which accounts for only a small fraction of the composition.

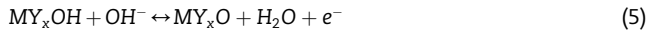
X-ray photoelectron spectroscopy is another essential method to analyze the composition of materials. The XPS spectra of the  $\text{Co}_3\text{O}_4/\text{MoS}_2$  composite is exhibited in Fig. 4. The result shows the presence of molybdenum, sulfur, cobalt, and oxygen elements. Firstly, the spectrum of  $\text{Co} 2p$  is shown in Fig. 4a, which shows two dipoles with a binding capacity of 779.3 eV and 795.4 eV, corresponding to the spin-orbit coupling levels of  $\text{Co} 2p_{3/2}$  and  $\text{Co} 2p_{1/2}$ , respectively [23–25]. Secondly, Fig. 4b shows the combined energy spectrum of  $\text{O} 1s$ , where the peak value of 529.9 eV can be attributed to the surface lattice  $\text{O}^{2-}$  of the metal oxide. Besides, the peak value of 531.1 eV corresponds to the adsorption of oxygen and hydroxyl. These results confirm that  $\text{Co}_3\text{O}_4$  is the primary cobalt source in the composite rather than  $\text{CoO}$ . Fig. 4c shows the  $\text{Mo} 3d$  spectrogram of the composite material, which has three peaks corresponding to  $\text{Mo}$  and  $\text{S}$  species existing in the sample. The peaks at 233.05 and 229.9 eV are  $\text{Mo} 3d_{3/2}$  and  $\text{Mo} 3d_{5/2}$  binding energies, respectively. These peaks can be attributed to the  $\text{Mo}^{4+}$ , which confirms  $\text{MoS}_2$  nanowires' formation. The peak at 227.05 eV can be attributed to the  $\text{S}$  element's  $2s$  binding energy in  $\text{MoS}_2$ . Finally, the high-resolution  $\text{S} 2p$  spectrum shows the analytical peaks at 161.9 eV and 163.3 eV in Fig. 4d, which can correspond to the spin orbits of  $\text{S} 2p_{3/2}$  and  $\text{S} 2p_{1/2}$ , respectively. These binding energies are consistent with the other reported  $\text{MoS}_2$  crystal data [26,27].

The electrochemical properties of the  $\text{Co}_3\text{O}_4/\text{MoS}_2$  composite were evaluated by three-electrode electrochemical tests in the range of 0–0.4 V potential. Fig. 5a shows cyclic voltammetry (CV) curves of  $\text{Co}_3\text{O}_4/\text{MoS}_2$  composites at different scanning rates (5–100 mV s<sup>-1</sup>). As can be seen from the figure, with the increase of the scanning rate, the CV curve of the composite material shows a strong current response,

indicating that the  $\text{Co}_3\text{O}_4/\text{MoS}_2$  composite material has excellent capacitance characteristics. CV curve has a large deviation from the rectangle, and there are obvious redox peaks. It reflects that the redox reaction occurred in the charging and discharging process, and the composite has typical pseudocapacitance property. Simultaneously, when the electron flow rate is greater than the reaction rate, the polarization effect will be generated. With the increase of the scanning rate, the CV curve will move the anode peak to the direction of high potential and the cathode peak to low potential [28]. Other literature has reported similar curve shapes [29–31]. Compared with the CV curve of raw  $\text{Co}_3\text{O}_4$  material, as shown in supporting information Fig. S1, its effective area has been significantly increased, which proves that the specific capacitance of the material has been greatly improved. According to the report, the redox reaction peak in Fig. 5a corresponds to the redox reaction of  $\text{Co}_3\text{O}_4$  and  $\text{MoS}_2$  with  $\text{OH}^-$  in electrolyte. The  $\text{Co}_3\text{O}_4$  reaction equations were as follows:



And according to recent reports by Barik et al. [32,33],  $\text{MoS}_2$  may react with the electrolyte as follows:



Where  $\text{MY}_x$  is layered sulfide and non-layered sulfide (including:  $\text{MoS}_2$ ,  $\text{WS}_2$ ,  $\text{FeS}_2$ , etc.). Fig. 5b displays the galvanostatic charge/discharge (GCD) test results of  $\text{Co}_3\text{O}_4/\text{MoS}_2$  composite powder with different current densities in KOH solution (6m) at 0–0.4 V (relative to SCE). These curves have distinct slopes at different current densities. Therefore, the material exhibits typical pseudocapacitance characteristics. Moreover, compared with the GCD curve of raw  $\text{Co}_3\text{O}_4$  (shown in supporting information Fig. S2), the discharge time at the same current density is significantly prolonged, which confirms the increase of material capacitance and is consistent with the test results in Fig. 5a. Formula  $C = It / \Delta Vm$  was used to calculate the specific capacitance at different current densities.  $I$  is the discharge current,  $t$  is the total discharge time,  $\Delta V$  is the potential drop in the discharge process, and  $m$  was the mass of  $\text{Co}_3\text{O}_4/\text{MoS}_2$ . The calculated results are shown as well as the specific capacitance of raw  $\text{Co}_3\text{O}_4$  and coulombic efficiency of  $\text{Co}_3\text{O}_4/\text{MoS}_2$  in Fig. 5c. When the current density is 0.5, 1, 2, 5 and 10 A g<sup>-1</sup>, the specific capacitance of the  $\text{Co}_3\text{O}_4/\text{MoS}_2$  composite material is 337, 335, 332, 320.5 and 310.3 F g<sup>-1</sup>, and the coulomb efficiency is 97.48%, 98.12%, 98.57%, 99.12% and 99.45%, respectively. However, when the current density is the same, the original  $\text{Co}_3\text{O}_4$  material's specific capacitance is only 53.25, 46.25, 41.25, 37.5, and 33.5 F g<sup>-1</sup>, respectively. The data showed that by coating the  $\text{Co}_3\text{O}_4$  powder with an outer layer of  $\text{MoS}_2$ , the material's specific capacitance increased more than six times. Besides, cyclic stability is another important property of electrode materials for supercapacitors. Finally, the cyclic stability of  $\text{Co}_3\text{O}_4/\text{MoS}_2$  composite material, 2000 charge, and discharge cycles were performed at the current density of 10 A g<sup>-1</sup>. The cyclic test results are shown in

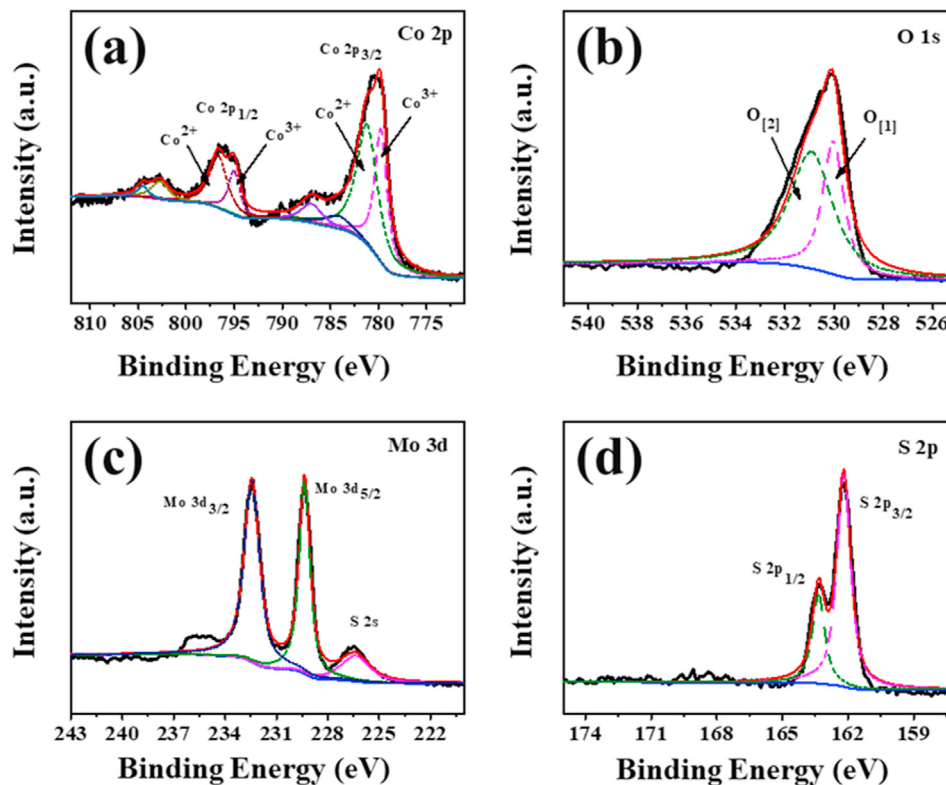


Fig. 4 – XPS survey spectra of  $\text{Co}_3\text{O}_4/\text{MoS}_2$  composite; (a) Co 2p; (b) O 1s; (c) Mo 3d; (d) S 2p.

Fig. 5d. Moreover, it indicated that after 2000 cycles of charging and discharging, the material's specific capacitance is still 93.6%, so it has excellent cycle stability and long service life.

Through experiments and data analysis,  $\text{Co}_3\text{O}_4/\text{MoS}_2$  with a core–shell structure has several times more noticeable performance improvement than the original  $\text{Co}_3\text{O}_4$  powder. We analyze that this is not only due to the mechanical

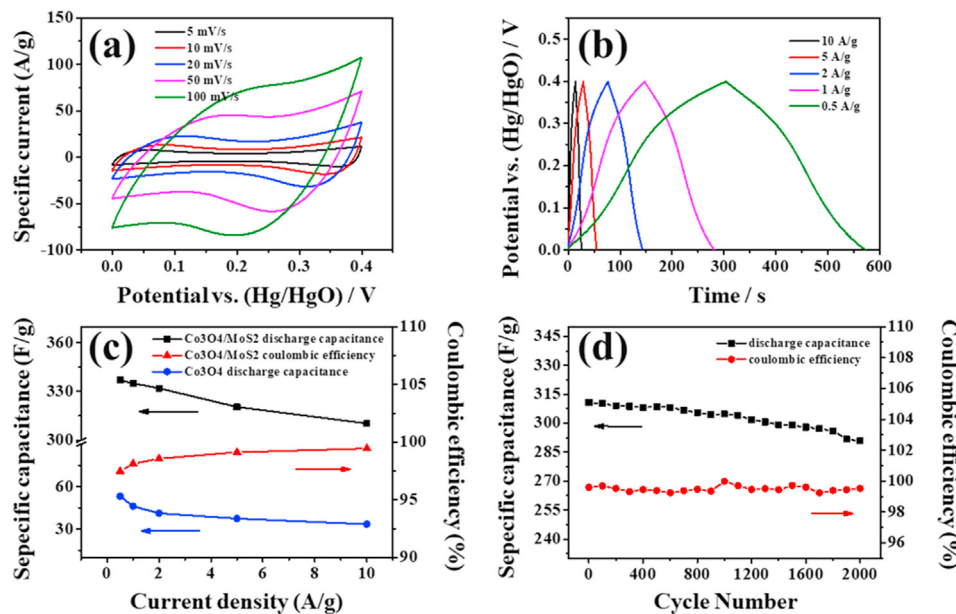


Fig. 5 – (a) CV curves of the  $\text{Co}_3\text{O}_4/\text{MoS}_2$  composite at different scan rates; (b) Galvanostatic charge–discharge curves of the  $\text{Co}_3\text{O}_4/\text{MoS}_2$  composite at various current densities; (c) Specific capacitance and Coulomb efficiency of  $\text{Co}_3\text{O}_4/\text{MoS}_2$  composites at different current densities, and comparison with a specific capacitance of  $\text{Co}_3\text{O}_4$  raw materials; (d) Capacitance retention of the  $\text{Co}_3\text{O}_4/\text{MoS}_2$  composite electrodes after 2000 cycles at a current density of  $10 \text{ A g}^{-1}$ .

combination of  $\text{Co}_3\text{O}_4$  and  $\text{MoS}_2$ , but also due to the following mutual enhancement effect:(a) The  $\text{MoS}_2$  nanowires on  $\text{Co}_3\text{O}_4$  shorten the transport/diffusion path of electrons and ions, resulting in a faster kinetic. (b) The lamellar structure of  $\text{MoS}_2$  and the weak van der Waals interaction between layers facilitate the adsorption and desorption of electrons and provide a full reaction surface and a larger internal space, promoting the sufficient contact between active substances and electrolytes. (c) In charging and discharging, the outer layer of the  $\text{MoS}_2$  nanometer sheet can buffer the volume expansion of  $\text{Co}_3\text{O}_4$  powder inside. Therefore, the electrochemical properties of  $\text{Co}_3\text{O}_4/\text{MoS}_2$  composites have been improved significantly.

#### 4. Conclusions

In summary,  $\text{Co}_3\text{O}_4/\text{MoS}_2$  core–shell composites with high electrochemical properties were prepared through a simple one-step MPCVD method by wrapping the  $\text{MoS}_2$  nanometer sheet on the surface of spherical  $\text{Co}_3\text{O}_4$  powder. The experiment equipment is refitted by the household microwave oven, which is simple to operate, low cost, short time consuming, and has a remarkable effect. A series of tests and analyses confirmed that the vertical flake  $\text{MoS}_2$  nanometer sheet layer was synthesized on  $\text{Co}_3\text{O}_4$  powder's surface and its surface morphology, composition structure, elemental valence state, and electrochemical performance were studied. The test results show that the specific capacitance of the  $\text{Co}_3\text{O}_4/\text{MoS}_2$  composite material can reach  $337 \text{ F g}^{-1}$  at the highest, with excellent multiplier performance and cycle stability. It could maintain 93.6% of the initial specific capacitance after 2000 following charges and discharges. Finally, according to the test results, the composite material's performance improvement compared with the raw material is analyzed. This paper presents an idea of combining extensive particle powder with nanometer sheet material, which can achieve high specific capacitance and maintain excellent cycling stability.

#### Declaration of Competing Interest

We declare that we have no financial and personal relationships with other people or organizations that can inappropriately influence our work, there is no professional or other personal interest of any nature or kind in any product, service and/or company that could be construed as influencing the position presented in, or the review of, the manuscript entitled “Efficient and inexpensive MPCVD method to synthesize  $\text{Co}_3\text{O}_4/\text{MoS}_2$  heterogeneous composite materials with high stability for supercapacitors”.

#### Acknowledgements

This work is supported by National Natural Science Foundation of China (51864028); Yunnan Province Science and Technology Major Project for Materials Genetic Engineering of

Rare and Precious Metal (202002AB080001), Applied Basic Research Fund Project of Yunnan Province (2018FD053, 2018FA029); Yunnan Province Funds for Distinguished Young Scientists (No. 2019FJ005); Yunnan Province Ten Thousand Talents Plan Young & Elite Talents Project (No. YNWRQNB-2018-311).

#### Appendix A. Supplementary data

Supplementary data to this article can be found online at <https://doi.org/10.1016/j.jmrt.2020.12.101>.

#### REFERENCES

- [1] Yuan SG, Pang SY, Hao JH. 2D transition metal dichalcogenides, carbides, nitrides, and their applications in supercapacitors and electrocatalytic hydrogen evolution reaction. *Appl Phys Rev* 2020;7:021304.
- [2] Zhang LY, Shi DW, Liu T, Jaroniec M, Yu JG. Nickel-based materials for supercapacitors. *Mater Today* 2019;25:35–65.
- [3] Huang TT, Jiang Y, Shen GZ, Chen D. Recent advances of two-dimensional nanomaterials for electrochemical capacitors. *ChemSusChem* 2020;13:1093–113.
- [4] Hou RL, Liu B, Sun YL, et al. Recent advances in dual-carbon based electrochemical energy storage devices. *Nano Energy* 2020;72:104728.
- [5] Liu G, Kang CX, Fang J, Fu LK, Zhou HH, Liu QM.  $\text{MnO}_2$  nanosheet-coated  $\text{Co}_3\text{O}_4$  complex for 1.4 V extra-high voltage supercapacitors electrode material. *J Power Sources* 2019;431:48–54.
- [6] Zhai T, Wan LM, Sun S, et al. Phosphate ion functionalized  $\text{Co}_3\text{O}_4$  ultrathin nanosheets with greatly improved surface reactivity for high performance pseudocapacitors. *Adv Mater* 2017;29:1604167.
- [7] Zheng YC, Lia ZQ, Xu J, et al. Multi-channeled hierarchical porous carbon incorporated  $\text{Co}_3\text{O}_4$  nanopillar arrays as 3D binder-free electrode for high performance supercapacitors. *Nano Energy* 2016;20:94–107.
- [8] Zhao X, Mao L, Cheng QH, et al. Two-dimensional spinel structured Co-based materials for high performance supercapacitors: a critical review. *Chem Eng J* 2020;387:124081.
- [9] Li SM, Yang K, Ya P, Ma KR, Zhang Z, Huang Q. Three-dimensional porous carbon/ $\text{Co}_3\text{O}_4$  composites derived from graphene/Co-MOF for high performance supercapacitor electrodes. *Appl Surf Sci* 2020;503:144090.
- [10] Han DD, Wei JH, Zhao Y, et al. Metal-organic framework derived petal-like  $\text{Co}_3\text{O}_4@\text{CoNi}_2\text{S}_4$  hybrid on carbon cloth with enhanced performance for supercapacitors. *Inorg Chem Front* 2020;7:1428–36.
- [11] Bao YX, Deng Y, Wang MZ, et al. A controllable top-down etching and in-situ oxidizing strategy: metal-organic frameworks derived alpha- $\text{Co}/\text{Ni(OH)}_2@\text{Co}_3\text{O}_4$  hollow nanocages for enhanced supercapacitor performance. *Appl Surf Sci* 2020;504:144395.
- [12] Bao L, Li T, Chen S, et al. 3D graphene frameworks/ $\text{Co}_3\text{O}_4$  composites electrode for high-performance supercapacitor and enzymeless glucose detection. *Small* 2017;13:1602077.
- [13] Shi ZJ, Xing L, Liu Y, Gao YF, Liu JR. A porous biomass-based sandwich-structured  $\text{Co}_3\text{O}_4@\text{Carbon Fiber}@/\text{Co}_3\text{O}_4$  composite for high-performance supercapacitors. *Carbon* 2018;129:819–25.

- [14] Guan C, Sumboja A, Wu HJ, et al. Hollow  $\text{Co}_3\text{O}_4$  nanosphere embedded in carbon arrays for stable and flexible solid-state zinc-air batteries. *Adv Mater* 2017;29:1704117.
- [15] Wang S, Wang T, Shi Y, Liu G, Li JP. Mesoporous  $\text{Co}_3\text{O}_4$ @carbon composites derived from microporous cobalt-based porous coordination polymers for enhanced electrochemical properties in supercapacitors. *RSC Adv* 2016;6:18465–70.
- [16] Zhao ZT, Zhang J, Wang WD, et al. Synthesis and electrochemical properties of  $\text{Co}_3\text{O}_4$ -rGO/CNTs composites towards highly sensitive nitrite detection. *Appl Surf Sci* 2019;485:274–82.
- [17] Chen YJ, Wang YS, Wang ZP, et al. Densification by compaction as an effective low-cost method to attain a high areal lithium storage capacity in a CNT@ $\text{Co}_3\text{O}_4$  sponge. *Adv Energy Mater* 2018;8:1702981.
- [18] Jia WL, Li J, Lu ZJ, Juan YF, Jiang YQ. Synthesis of porous  $\text{Co}_3\text{O}_4$ /Reduced graphene oxide by a two-step method for supercapacitors with excellent electrochemical performance. *J Alloys Compd* 2020;815:152373.
- [19] Yin XJ, Zhi CW, Sun WW, Lv LP, Wang Y. Multilayer  $\text{NiO}@\text{Co}_3\text{O}_4$ @graphene quantum dots hollow spheres for high-performance lithium-ion batteries and supercapacitors. *J Mater Chem A* 2019;7:7800–14.
- [20] Wang JP, Zhou H, Zhu MZ, Yuan AH, Shen XP. Metal-organic framework-derived  $\text{Co}_3\text{O}_4$  covered by  $\text{MoS}_2$  nanosheets for high-performance lithium-ion batteries. *J Alloys Compd* 2018;744:220–7.
- [21] Liu Y, Sun J, Lin SY, Xu ZK, Li L. In-situ growth of interconnected  $\text{NiS}_2/\text{MoS}_2$  nanowires supported on Ni foam as binder-free electrode for hybrid supercapacitor. *J Alloys Compd* 2020;820:153113.
- [22] Zhang HH, Wei J, Yan Y, et al. Facile and scalable fabrication of  $\text{MnO}_2$  nanocrystallines and enhanced electrochemical performance of  $\text{MnO}_2/\text{MoS}_2$  inner heterojunction structure for supercapacitor application. *J Power Sources* 2020;450:227616.
- [23] Zhang LM, Yan B, Zhang JH, Liu YJ, Yuan AH, Yang G. Design and self-assembly of metal-organic framework-derived porous  $\text{Co}_3\text{O}_4$  hierarchical structures for lithium-ion batteries. *Ceram Int* 2016;42:5160–70.
- [24] Wang Y, Wang CY, Wang YJ, Liu HK, Huang ZG. Superior sodium-ion storage performance of  $\text{Co}_3\text{O}_4$ @nitrogen-doped carbon: derived from a metal-organic framework. *J Mater Chem A* 2016;4:5428–35.
- [25] Liang DW, Tian ZF, Liu J, et al.  $\text{MoS}_2$  nanosheets decorated with ultrafine  $\text{Co}_3\text{O}_4$  nanoparticles for high-performance electrochemical capacitors. *Electrochim Acta* 2015;182:376–82.
- [26] Liang YL, Feng RJ, Yang SQ, Ma H, Liang J, Chen J. Rechargeable Mg batteries with graphene-like  $\text{MoS}_2$  cathode and ultrasmall Mg nanoparticle anode. *Adv Mater* 2011;23:640–3.
- [27] Lin HT, Chen XY, Li HL, Yang M, Qi YX. Hydrothermal synthesis and characterization of  $\text{MoS}_2$  nanorods. *Mater Lett* 2010;64:1748–50.
- [28] Tummala R, Guduru RK, Mohanty PS. Nanostructured  $\text{Co}_3\text{O}_4$  electrodes for supercapacitor applications from plasma spray technique. *J Power Sources* 2012;209:44–51.
- [29] Ge X, Gu CD, Wang XL, Tu JP. Correlation between microstructure and electrochemical behavior of the mesoporous  $\text{Co}_3\text{O}_4$  sheet and its ionothermal synthesized hydrotalcite-like alpha- $\text{Co(OH)}_2$  precursor. *J Phys Chem C* 2014;118:911–23.
- [30] Zhang HN, Chen YJ, Wang WW, et al. Hierarchical Mo-decorated  $\text{Co}_3\text{O}_4$  nanowire arrays on Ni foam substrates for advanced electrochemical capacitors. *J Mater Chem A* 2013;1:8593–600.
- [31] Dong XC, Xu H, Wang XW, et al. 3D graphene-cobalt oxide electrode for high-performance supercapacitor and enzymeless glucose detection. *ACS Nano* 2012;6:3206–13.
- [32] Barik R, Ingole PP. Challenges and prospects of metal sulfide materials for supercapacitors. *Curr Opin Electrochem* 2020;21:327–34.
- [33] Sanchez JS, Pendashteh A, Palma J, Anderson M, Marcilla R. Insights into charge storage and electroactivation of mixed metal sulfides in alkaline media: NiCoMn ternary metal sulfide nano-needles forming core-shell structures for hybrid energy storage. *J Mater Chem A* 2019;7:20414–24.